environmental microbiology

Environmental Microbiology (2013) doi:10.1111/1462-2920.12241

Community differentiation and population enrichment of Sargasso Sea bacterioplankton in the euphotic zone of a mesoscale mode-water eddy

Craig E. Nelson,[1,2]* Craig A. Carlson,[1] Courtney S. Ewart[1] and Elisa R. Halewood[1]

[1]*Marine Science Institute and Department of Ecology, Evolution and Marine Biology, University of California, Santa Barbara, CA 93106, USA.*

[2]*Center for Microbial Oceanography: Research and Education (C-MORE), Department of Oceanography, University of Hawai'i at Mānoa, Honolulu, HI 96822, USA.*

Summary

Eddies are mesoscale oceanographic features (~ 200 km diameter) that can cause transient blooms of phytoplankton by shifting density isoclines in relation to light and nutrient resources. To better understand how bacterioplankton respond to eddies, we examined depth-resolved distributions of bacterial populations across an anticyclonic mode-water eddy in the Sargasso Sea. Previous work on this eddy has documented elevated phytoplankton productivity and diatom abundance within the eddy centre with coincident bacterial productivity and biomass maxima. We illustrate bacterial community shifts within the eddy centre, differentiating populations uplifted along isopycnals from those enriched or depleted at horizons of enhanced bacterial and primary productivity. Phylotypes belonging to the Roseobacter, OCS116 and marine Actinobacteria clades were enriched in the eddy core and were highly correlated with pigment-based indicators of diatom abundance, supporting developing hypotheses that members of these clades associate with phytoplankton blooms. Typical mesopelagic clades (SAR202, SAR324, SAR406 and SAR11 IIb) were uplifted within the eddy centre, increasing bacterial diversity in the lower euphotic zone. Typical surface oligotrophic clades (SAR116, OM75, Prochlorococcus and SAR11 Ia) were relatively depleted in the eddy centre. The biogeochemical context of a bloom-inducing eddy provides insight into the ecology of the diverse uncultured bacterioplankton dominating the oligotrophic oceans.

Received 9 May, 2013; revised 9 July, 2013; accepted 1 August, 2013. *For correspondence. E-mail craig.nelson@hawaii.edu; Tel. (+805) 705 3497; Fax (+808) 956 9225.

Introduction

Determining the factors that regulate the composition of diverse microbial communities in nature is one of the central challenges in ecology today. Examining changes in microbial populations in response to disturbance along well-characterized environmental gradients provides a snapshot into the ways in which microbial communities shift in response to environmental change, and can simultaneously enhance our understanding of the biogeochemical relevance of shifts in community structure (Carlson *et al.*, 2008; Nelson, 2009; Giovannoni and Vergin, 2012). Pelagic bacteria in the euphotic zone of the oligotrophic subtropical gyres play a major role in the biogeochemistry and food web dynamics of the open ocean (Ducklow, 1999), and understanding how these communities respond to physical and biological forcing is central to developing a predictive understanding of the linkages between bacterial taxa and biogeochemical cycling.

Mesoscale eddies (~ 200 km diameter), found commonly in the oligotrophic gyres, have been implicated in spatially and temporally transient pulses of nutrient input, enhanced primary productivity, changes in phytoplankton community structure and vertical export of organic matter (McGillicuddy *et al.*, 1999; 2007; Siegel *et al.*, 1999). The physical dynamics associated with mid-ocean cyclonic eddies and anticyclonic mode-water eddies (MWEs) produce isopycnal uplift of the seasonal thermocline that can lead to nutrient delivery and enhanced biological productivity in the euphotic zone of oligotrophic systems. It has been hypothesized that the enhanced biological activity associated within these mesoscale features helps to close the gap between traditional estimates of net community production in oligotrophic subtropical gyres (Eppley and Peterson, 1979) and more modern tracer-based estimates (Jenkins *et al.*, 1988; 2008; Jenkins and Doney, 2003).

MWEs within the Sargasso Sea are distinguished by a doming of the shallower seasonal thermocline but a depression of the deeper permanent thermocline by lateral advection of 18°C water (known as 'mode-water')

from the gyre edges (Richardson, 1993; McGillicuddy *et al*., 1999; Siegel *et al*., 1999). Because MWEs are anticyclonic in rotation, they combine doming of the seasonal nutricline into the euphotic zone with wind interaction that can result in significant diatom productivity for several months (Bibby *et al*., 2008). The enhanced productivity is attributed to vertical advection and turbulent diffusion of nutrients because of eddy–wind interactions (McGillicuddy *et al*., 2007; Ledwell *et al*., 2008). The eddy studied here (MWE 'A4') exhibited a positive sea-level anomaly of ~ 20 cm and was at least 4 months old at the time of sampling. Despite its age, the eddy exhibited elevated primary production with diatom pigment concentrations more than 8 standard deviations above the Bermuda Atlantic Time Series (BATS) mean (McGillicuddy *et al*., 2007). Ewart and colleagues (2008) demonstrated enhanced bacterial production (BP) in the centre of the eddy spatially coincident with elevated levels of chlorophyll, primary productivity and diatom-associated pigments, suggesting that specific bacterioplankton community adaptations may be occurring in response to enhanced primary productivity.

The goal of the present study was to understand how the diverse bacterioplankton populations of the Sargasso Sea may respond to transient eddy events, particularly the enhanced productivity and altered phytoplankton communities observed in MWEs such as A4. Our current understanding of the processes maintaining the diversity of bacterioplankton in the open ocean is limited, but observations and theory suggest that specific populations may be adapted to respond to spatially and temporally heterogeneous pulses of photosynthetic productivity (copiotrophs) while others are adapted to steady-state resource-depleted conditions (oligotrophs; Lauro *et al*., 2009; Giovannoni and Vergin, 2012; Nelson and Carlson, 2012). We hypothesized that populations previously associated with particle-attached lifestyles, elevated nutrients or senescing diatoms would be enhanced within the eddy core in response to the elevated production, whereas many of the numerically dominant oligotrophic clades found in the Sargasso Sea (Giovannoni and Vergin, 2012) may become relatively depleted within the eddy core because of poor competitive dominance under elevated nutrient delivery. Given the physical structure of eddies, we anticipated a second, abiotic driver of community differentiation within the eddy caused by the isopycnal uplift of mesopelagic waters into the euphotic zone via eddy vorticity. Because the greatest differences in Sargasso bacterioplankton communities occur at the transition from euphotic to mesopelagic depth horizons (Morris *et al*., 2005; Treusch *et al*., 2009), we hypothesized that there would be a distinct phylogenetic difference between those taxa which are displaced vertically and those that exhibit localized increases or decreases only within the eddy core in response to the enhanced nutrient delivery and productivity (i.e. 'blooms').

To test these hypotheses, we surveyed bacterial community structure along 11 euphotic zone depth profiles (40–120 m) collected synoptically within and adjacent to a mesoscale eddy feature during two occupations of anticyclonic MWE A4 in July–August of 2005 (McGillicuddy *et al*., 2007; Ewart *et al*., 2008) as well as an outside comparative station at the BATS site roughly 100 km northeast of the eddy edge. Population distributions within and outside of the eddy centre were analysed via relative abundances of pyrosequenced amplicons of the V1-V2 regions of the 16S ribosomal RNA gene in DNA extracted from water via 0.2 μm filtration. These community profiles allow us to present both visual displays of bacterioplankton population depth distributions across the euphotic zone of an active MWE transect and also rigorously test for statistical differences in depth distributions of each population within and outside of the eddy core. Placing these community shifts in the context of the comprehensive physical, chemical and biological data collected synoptically allows us to propose linkages between biogeochemical processes and the transient dynamics of bacterioplankton populations in the open ocean.

Results

Eddy physical and biogeochemical characteristics

Previous work has detailed much of the physical structure and biogeochemical response of MWE A4, compiled in a single topical volume of the journal *Deep Sea Research II* (Benitez-Nelson and McGillicuddy, 2008), including vertical nutrient flux (Ledwell *et al*., 2008; Li and Hansell, 2008), plankton response (Bibby *et al*., 2008; Ewart *et al*., 2008; Goldthwait and Steinberg, 2008) and particle flux (Buesseler *et al*., 2008). The eddy core exhibited a persistent deep fluorescence maximum between 80 and 100 m coincident with elevated primary and BP, increased vertical flux of inorganic nutrients and elevated diatom abundance (McGillicuddy *et al*., 2007).

To determine if bacterial community composition showed coincident responses to the eddy perturbation, we contrasted measurements of population distributions in the centre of the eddy with those at the eddy edges and nearby BATS site (out station). To objectively define each of the 22 profiles (Fig. 1) as being within or outside the eddy centre, we clustered samples collected at 100 m depth according to potential density (σ_θ) and dissolved inorganic nitrogen concentrations (DIN; nitrate + nitrite). Samples fell into two distinct groups (Fig. 2) consistent with the distance-based classifications of Ewart and colleagues (2008), where eddy centre and eddy edge were defined as hydrographic stations < 20 km and > 25 km of the point of minimum velocity, respectively,

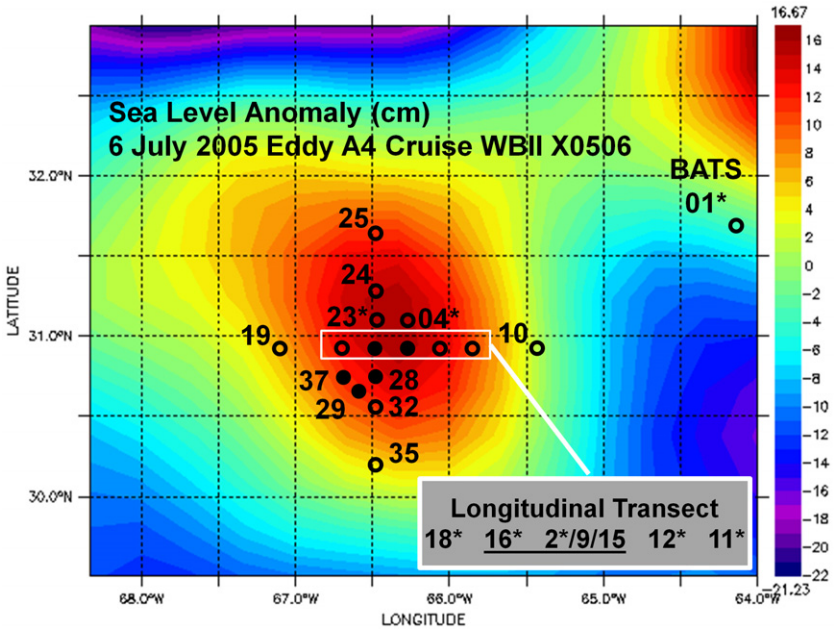

Fig. 1. Surface map of 22 sampling stations on R/V Weatherbird cruise X0506 6–15 July 2005. Points are profile locations labelled with cast code number (see Fig. 2 for a complete list of profiles). Solid symbols denote samples classified as eddy centre. Asterisks denote samples analysed for bacterial community structure with 16S pyrosequencing ($n = 11$). Not shown are three eddy centre casts from a second occupation of the eddy 16–25 August 2005 which were also analysed with 16S pyrosequencing. Note that casts 09 and 15 are spatially coincident with cast 02 but temporally offset by 1 and 3 days respectively. Map of sea surface topography from NOAA/PMEL AVISO Live Access Server: http://las.aviso.oceanobs.com.

as determined by acoustic Doppler current profiling. Just 1 of the 22 profiles was classified differently by the two methods (C28; Fig. 2); we maintain the previously published classifications of Ewart and colleagues (2008) herein for consistency with previous work.

Mean depth distributions of both potential density (Fig. 3A, $p_{e^*d} = 0.003$) and DIN (Fig. 3B, $p_{e^*d} = 0.006$) differed significantly between eddy centre and edge stations, with higher density isopycnals lifted above 100 m in the euphotic zone and enhanced DIN concentrations in

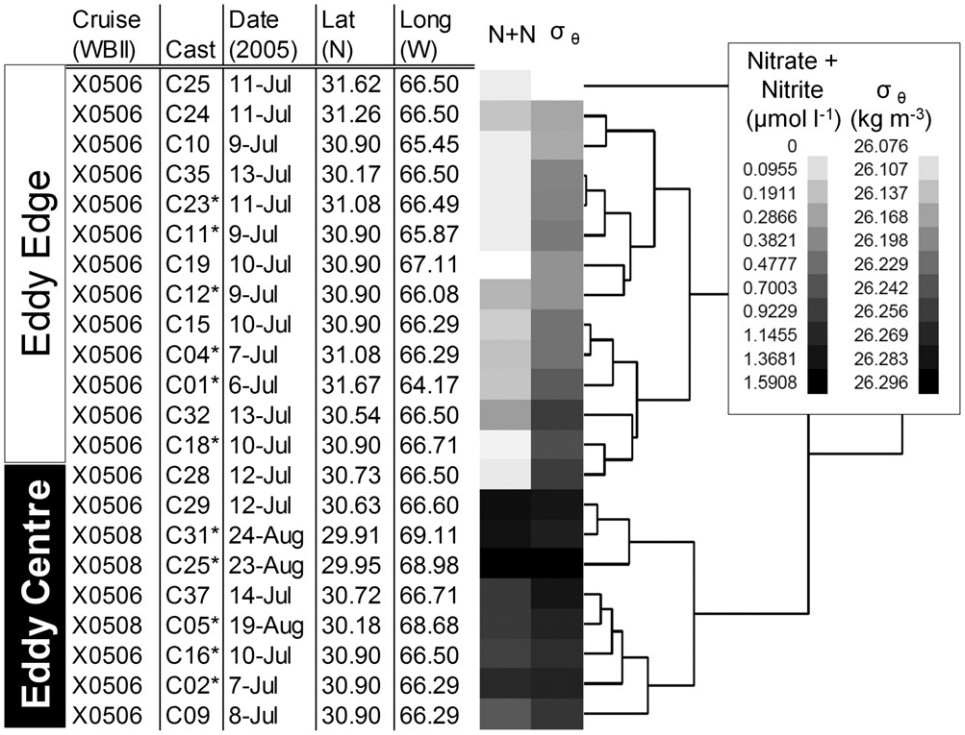

Fig. 2. Sampling locations and dates with differentiation of eddy centre and edge profiles according to water density and nitrogen concentration at the 100 m depth horizon. Dendrogram built using complete linkage hierarchical clustering on concentrations of nitrate plus nitrite (N + N) and potential density ($\sigma\theta$). Note the inclusion of three eddy centre samples from a second occupation of the same eddy on cruise WBII X0508 in August 2005. As in Fig. 1, casts marked with an asterisk ($n = 11$) were analysed for bacterial community composition via 16S pyrosequencing.

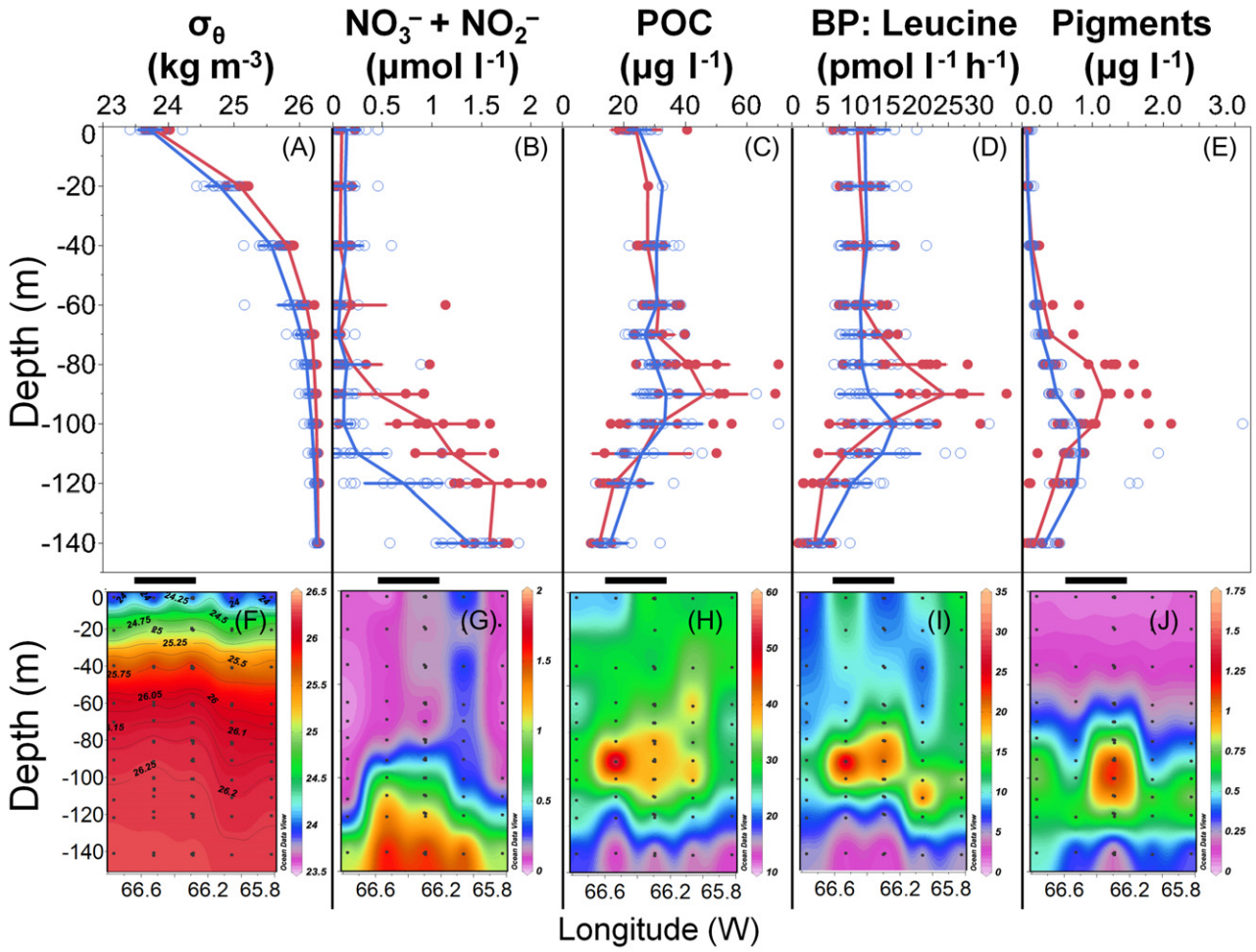

Fig. 3. Depth distributions of physical and biogeochemical parameters across the eddy over the upper 150 m. Top panels (A–E) show mean ± one standard deviation across all 22 sampling profiles classified according to eddy edge (blue; open circles) or eddy centre (red; closed circles). Bottom panels (F–J) show contour data across a five-station longitudinal transect (spatially mapped in Fig. 1) with dark bars denoting eddy centre stations. Warmer colours signify increasing values of each parameter. Variables are potential density (A), nitrate + nitrite concentration (B), particulate organic carbon (C), bacterial production via leucine incorporation (D) and total phytoplankton pigments via HPLC (E). All variables exhibit significantly different depth profiles between eddy edge and centre (see *Results*).

the lower euphotic zone (below 80 m). Temperatures, as well as both salinity and oxygen concentrations, were reduced throughout the eddy centre relative to the eddy edge across the 40–120 m depth horizon ($p_e < 0.03$; data not shown). Biologically, the eddy centre exhibited statistically significant enrichment of particulate organic carbon (POC) (Fig. 3C, $p_{e*d} = 0.043$), rates of BP (Fig. 3D, $p_{e*d} = 0.005$) and total high-pressure liquid chromatography (HPLC)-analysed phytoplankton pigments (Fig. 3E, $p_{e*d} = 0.011$) relative to edge stations, with the greatest differences found at the 80–100 m depth horizons. One unusual characteristic of the A4 eddy centre was that the maxima of total pigment concentration, POC and BP were all coincident between 80 and 100 m. This observation was distinct from a typical summer profile in the Sargasso Sea in which the maxima are generally vertically separated, with the POC and BP maxima found in the upper euphotic zone (between 40 and 60 m) and the pigment maximum found roughly 40–50 m deeper in the euphotic zone between 90 and 110 m (Steinberg *et al.*, 2001).

16S pyrosequencing and community differentiation within the eddy

Of the 22 stations analysed in this dataset, a total of 11 station profiles were selected for 16S amplicon pyrosequencing analysis of five depths each spanning the lower euphotic zone (40, 60, 80, 100 and 120 m). The pyrosequencing produced a total of 79 326 quality-filtered sequence reads with mean and median read lengths of 263 base pairs following de-noising and alignment trimming. An average of 1469 amplicons were sequenced from each of 54 samples (range 771–2458 reads per

sample); one sample did not amplify well (40 m C01-BATS; < 50 reads before quality filtering) and was excluded from further analysis. These sequences clustered into 3768 operational taxonomic units (OTUs) at the 95% sequence identity level, 1442 of which were represented by more than one sequence (i.e. non-singletons).

Weighted UniFrac distances between samples (calculated from a bootstrapped maximum-likelihood phylogeny containing one representative sequence for each OTU) ranged from 0.06 to 0.50 with a mean and median of 0.23. Community differentiation among samples between eddy centre and other stations increased with depth across the 11 profiles (Fig. 4). There was relatively minor variation in bacterioplankton community structure among 40 and 60 m samples (UniFrac distances < 0.15, Fig. 4A and B); but at 80, 100 and 120 m, there was a large difference between communities found in the eddy centre from those at the edge (UniFrac distances > 0.2, Fig. 4C–E). Analysis of similarity (ANOSIM) demonstrated statistically significant community differentiation between eddy edge and centre overall ($P < 0.001$), with depth-specific pairwise differentiation not significant at 40 m ($P = 0.08$) and 60 m ($P = 0.42$) but significant and increasing from 80 m ($R = 0.34$, $P = 0.03$) to 100 m ($R = 0.73$, $P = 0.002$) to 120 m ($R = 0.82$, $P = 0.002$). The BATS profile samples clustered consistently and significantly with samples from the eddy edge (Fig. 4B–E), indicating that the eddy centre samples were anomalous departures from a representative summertime Sargasso Sea bacterioplankton community.

We ordinated community samples using multidimensional scaling (MDS) to derive two orthogonal axes of community variability (Fig. 5A). Axis 1 separated samples primarily according to depth (Fig. 5A and B) and differentiation between eddy centre and eddy edge increased with depth along this axis (Fig. 5C). Along axis 1, the communities within the eddy centre are most similar to those of deeper depths at the eddy edge (Fig. 5B; e.g. 100 m centre samples lie parallel to 120 m edge samples along axis 1), suggesting that this axis of community variation tracks the physical displacement of mesopelagic waters (and associated bacterioplankton) into the deeper euphotic zone depths within the eddy centre (Fig. 5C). Differentiation along axis 2 occurs primarily within the 80–100 m depth horizons and does not increase consistently with depth (Fig. 5A and D). This localized effect, best visualized across the eddy transect contours (Fig. 5D), is primarily associated with the zones of elevated BP, POC and phytoplankton pigments. Importantly, MDS maximizes orthogonality (correlational independence) of axes, emphasizing that community shifts along axis 2 at these depth horizons are likely indicating processes independent of the effect of vertical displacement associated with axis 1.

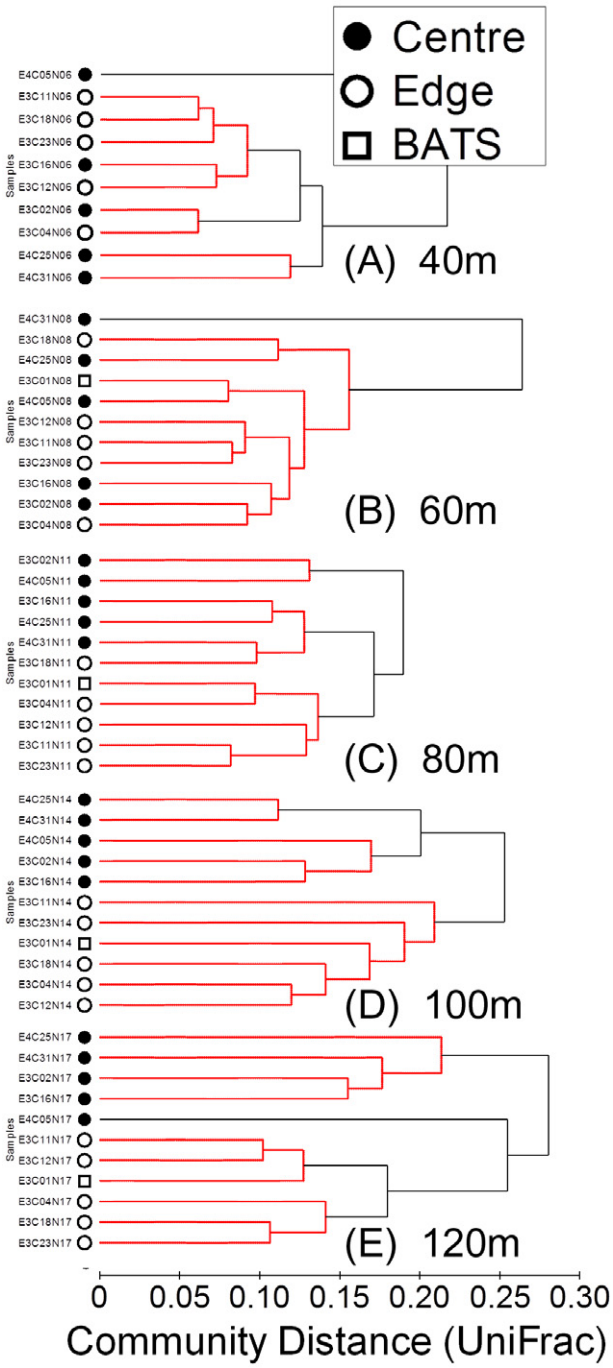

Fig. 4. Increasing community differentiation between eddy centre and eddy edge with depth. Hierarchical cluster dendrograms for each depth horizon (A–E) were generated from UniFrac community phylogenetic distances between samples. Samples are labelled according to cruise, cast and Niskin bottle and coded according to eddy centre (closed circles), eddy edge (open circles) or the BATS profile sample (open squares). Red lines denote samples which do not differ significantly by similarity profiling (SIMPROF; $\alpha = 0.05$).

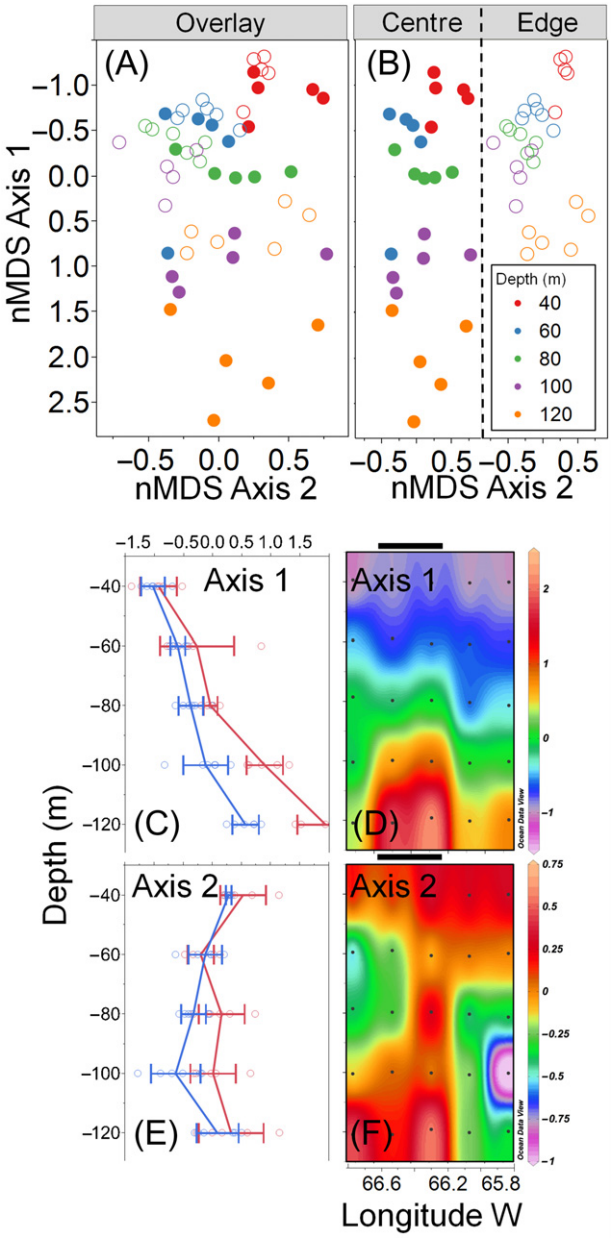

Fig. 5. Continuous community change over depth shows differences between physical displacement and eddy core differentiation. Results of multidimensional scaling ordination of samples according to 16S pyrosequencing-based UniFrac distance in bacterial phylogenetic structure. Panel (A) shows all samples ordinated together (stress = 0.12) and colour-coded by depth, with eddy centre as closed symbols and eddy edge as open symbols. Panel (B) uses the same ordination as (A), but presents eddy centre (left) and eddy edge (right) in separate plots to clarify the degree of differentiation with depth. Bottom panels (C–F) show depth distributions of the two orthogonal aspects of community structure [axis 1 (C and D); axis 2 (E and F)]. Panels C and E show depth profiles (mean ± one standard deviation) across all 11 sampling stations classified according to eddy edge (blue) or eddy centre (red). Contour plots (D and F) show depth distributions of each aspect of community structure across the five-profile longitudinal transect; dark bars denote eddy centre stations.

Bacterial diversity responses to the eddy

The number of OTUs observed by pyrosequencing ranged from 107 to 241 per sample after rarefaction by random subsampling at 700 sequences per sample; estimates of bacterial OTU richness ranged from 174 to 485 using the Chao1 metric (Chao, 1984) and from 240 to 2272 using the Catchall metric (Bunge, 2011); all sample diversity estimates are listed in Table S1. The depth distribution of observed OTU richness differed between eddy centre and edge, with increased richness below 80 m in the eddy centre [Fig. 6A; multivariate analysis of variance (MANOVA) $p_e = 0.0030$, $p_{e*d} = 0.0002$]. Diversity metrics also showed significantly elevated evenness (Pielou's *J*) and overall diversity (Shannon's *H*) within the eddy centre that increased with depth (Fig. 6C and D; MANOVA $p_e < 0.001$ and $p_{e*d} < 0.035$). We found no evidence of differences in pyrosequencing read acquisition between the eddy edge and eddy centre samples that might have biased these diversity analyses (MANOVA $p_e = 0.864$, $p_{e*d} = 0.153$).

Bacterial population responses within the eddy centre

To avoid statistical artefacts associated with multiple comparisons among thousands of OTUs, we limited population-level statistical analyses to a subset of 'common' OTUs ($n = 162$) defined strictly as being both abundant (> 0.02% or at least 15 sequences found across 54 samples) and widespread (multiple copies found in at least 2 samples). Representative sequences for each OTU were placed into a reference phylogenetic tree via the PhyloAssigner pipeline (Vergin *et al.*, 2013) to verify and further resolve consensus classifications; the classifications of all of these common OTUs and the complete results of statistical testing are listed in Table S2 with the complete reference tree (Vergin *et al.*, 2013) containing OTUs and scaffolded nearest neighbours from SILVA inserted in Fig. S1. Using MANOVA and controlling the false discovery rate, we identified a subset of 51 OTUs that exhibited significant differences in depth distributions between the eddy centre and eddy edge; as noted in the methods, we consider these a conservative estimate of those common taxa with consistent, resolvable responses to the eddy over multiple profiles. Of these, 22 showed only a significant between-subjects effect of eddy location (centre vs. edge, interpreted as profiles being consistently relatively enriched or depleted within the eddy across depths; $p_e < 0.013$, $q_e < 0.024$), 12 showed only a significant within-subjects interaction effect between depth and location (interpreted as differing in depth distributions within and outside of the eddy but not consistently enriched in either location; $p_{e*d} < 0.022$, $q_{e*d} < 0.035$) and 17 met significance criteria for both terms (i.e. significantly

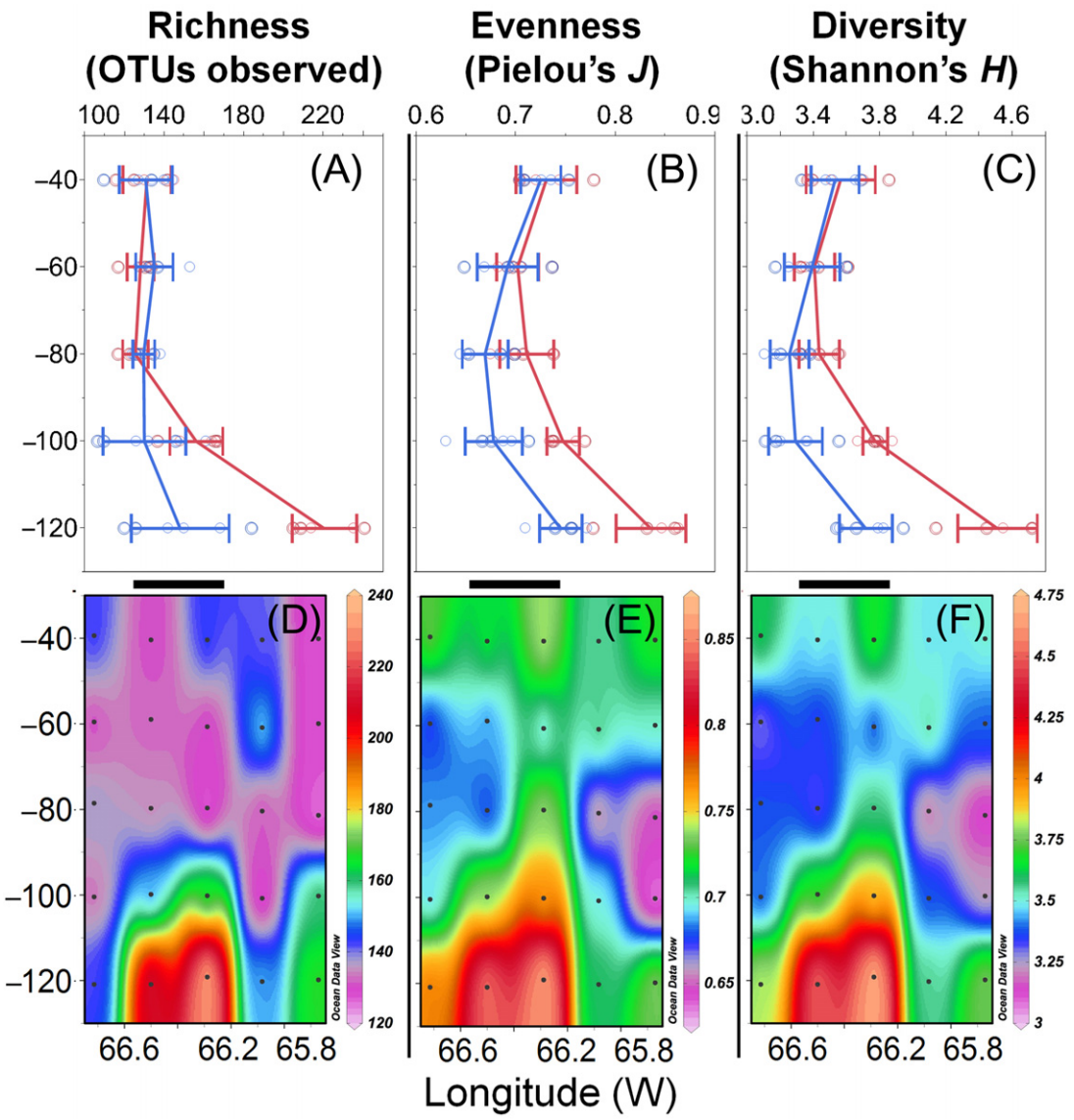

Fig. 6. Richness, evenness and diversity of bacterioplankton increase at depth within the eddy centre. Metrics are derived from 95% sequence identity operational taxonomic units (OTUs) from 16S pyrosequencing. Each panel includes depth distributions of each variable (mean ± one standard deviation) across all 11 sampling stations A–C classified according to eddy edge (blue) or eddy centre (red) with contour plots showing depth distributions of each variable across a five-station longitudinal transect (D–F); dark bars denote eddy centre stations. Profiles differ significantly between eddy edge and centre for all metrics via MANOVA (see *Results*).

relatively enriched or depleted within the eddy and with magnitude of difference varying by depth).

We have focused our subsequent analyses and discussion on a subset of 19 abundant OTUs (exceeding 1% of total sequences in at least two samples) for concision. All of these taxa were significantly affected by the eddy perturbation and belong to clades previously identified as being common within the Sargasso Sea ecosystem (Morris *et al*., 2004; 2005; Treusch *et al*., 2009; Giovannoni and Vergin, 2012). Based on depth distributions within and outside of the eddy centre (Fig. 7), we classified these taxa into three broad groups as follows. OTUs that were enriched at the eddy centre depths coincident with elevated primary and BP (Fig. 3) were labelled as 'enriched populations'. These OTUs were most pronounced within the 80–100 m depth horizon and included OTUs belonging to the Roseobacter OCT lineage (Buchan *et al*., 2005), OCS116, SAR86 and marine group Actinobacteria (OCS155, SVA0996) clades; most of these OTUs demonstrated a reduction in their relative abundance towards the base of the euphotic zone (Fig. 7, left column). OTUs that have previously been associated with a predominantly mesopelagic lifestyle (Morris *et al*., 2004; DeLong *et al*., 2006; Giovannoni and Vergin, 2012) and that

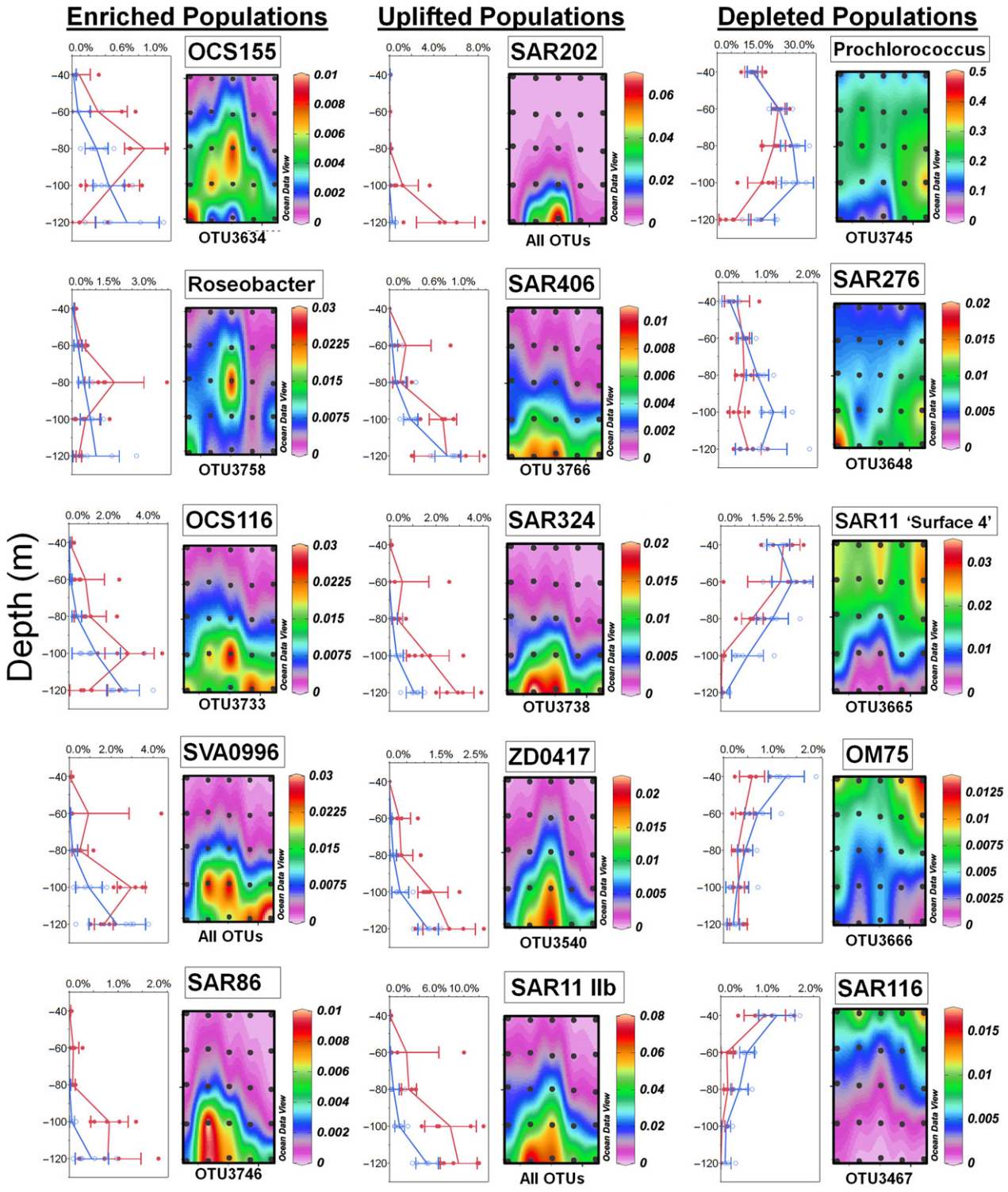

Fig. 7. Relative abundances of 15 selected dominant OTUs which differed significantly in depth distributions between eddy centre and eddy edge stations. Taxa are grouped according to proposed response to the eddy annotated at the top of each column. Each panel includes depth distributions of OTU relative abundance (mean ± one standard deviation) across all 11 sampling stations classified according to eddy edge (blue; open circles) or eddy centre (red; closed circles) with contour plots showing depth distributions across a five-profile longitudinal transect; dark bars denote eddy centre stations. Of the 19 abundant, significant OTUs just 15 plots are shown for concision: OTU3751 (SAR11 Ib) and OTU3752 (SAR11 Ia) were not plotted and three clades where all OTU representatives within the clades showed significant differences between eddy centre and eddy edge profiles, and the same spatial patterns (SAR202, SAR11 IIb and SVA0996) were combined into a complete phylotype distribution to more accurately represent abundance data, eliminating redundant plots.

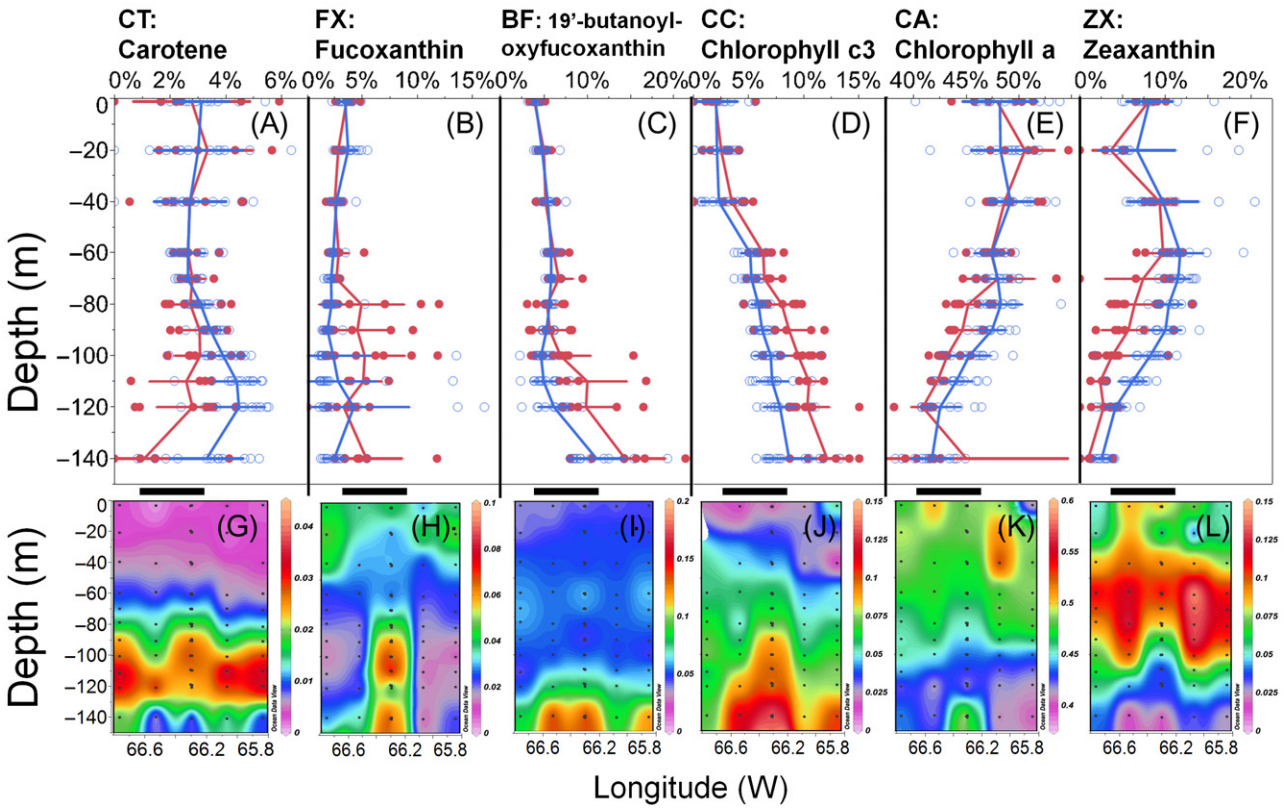

Fig. 8. Covariation between bacterial taxa and phytoplankton pigments which differed between eddy centre and eddy edge across mode-water eddy A4. Panels (A–F) show depth distributions of phytoplankton pigment relative abundances (mean ± one standard deviation) across all 22 sampling stations classified according to eddy edge (blue; open circles) or eddy centre (red; closed circles) with contour plots (G–L) showing depth distributions across a five-profile longitudinal transect; dark bars denote eddy centre stations. All pigments shown differed significantly between eddy edge and eddy centre by MANOVA (see *Results*).

demonstrated systematic relative enrichment at depth (base of the euphotic zone) were labelled as 'uplifted populations'; these included OTUs belonging to the SAR202 (cluster 3), SAR406, SAR324 Group I, SAR11 Group IIb and Gammaproteobacteria ZD0417 clades (Fig. 7, middle column). OTUs that exhibited a reduced relative abundance within the eddy centre were labelled as 'depleted populations' and included OTUs belonging to the Prochlorococcus, SAR11 Surface 4, SAR11 Group Ia, SAR116 Group Ia, OM75 and SAR276 clades (Fig. 7, right column).

Covariation between bacterial populations and phytoplankton pigments responding to the eddy

In order to more objectively judge the degree to which these dominant eddy-affected taxa differentially track phytoplankton communities, we developed a covariance matrix of Pearson's correlation coefficients between each of these 19 OTUs and the relative abundance of six phytoplankton pigments which differed significantly between eddy edge and eddy centre (Fig. 8; pigments used in covariance analysis were a subset selected from a total of 16 measured by HPLC and tested for significant eddy effects by MANOVA; $p_e < 0.05$). OTUs clustered into several distinct groups based on covariance patterns among the six eddy-affected pigments (Fig. 9), and these clusters corresponded well with the eddy response characteristics of the various OTUs organized in Fig. 7. OTUs belonging to the OCS116, Roseobacter and OCS155 clades showed the strongest correlation with fucoxanthin, an indicator of diatom abundance enriched primarily within the 80–100 m horizon of the eddy centre (Figs 8B and 9); the OTU belonging to OCS116 was additionally distinguished by a relatively strong association with β-carotene (Figs 8A and 9). In contrast, the depleted populations, including OTUs belonging to the SAR116 Group Ia, OM75, *Prochlorococcus* and SAR11 Group Ia & Surface 4, showed strong positive correlation with chlorophyll *a* and zeaxanthin concentrations (both of which were enriched outside of the eddy centre, Figs 8E and F) and relatively weak associations with other pigments (Fig. 9).

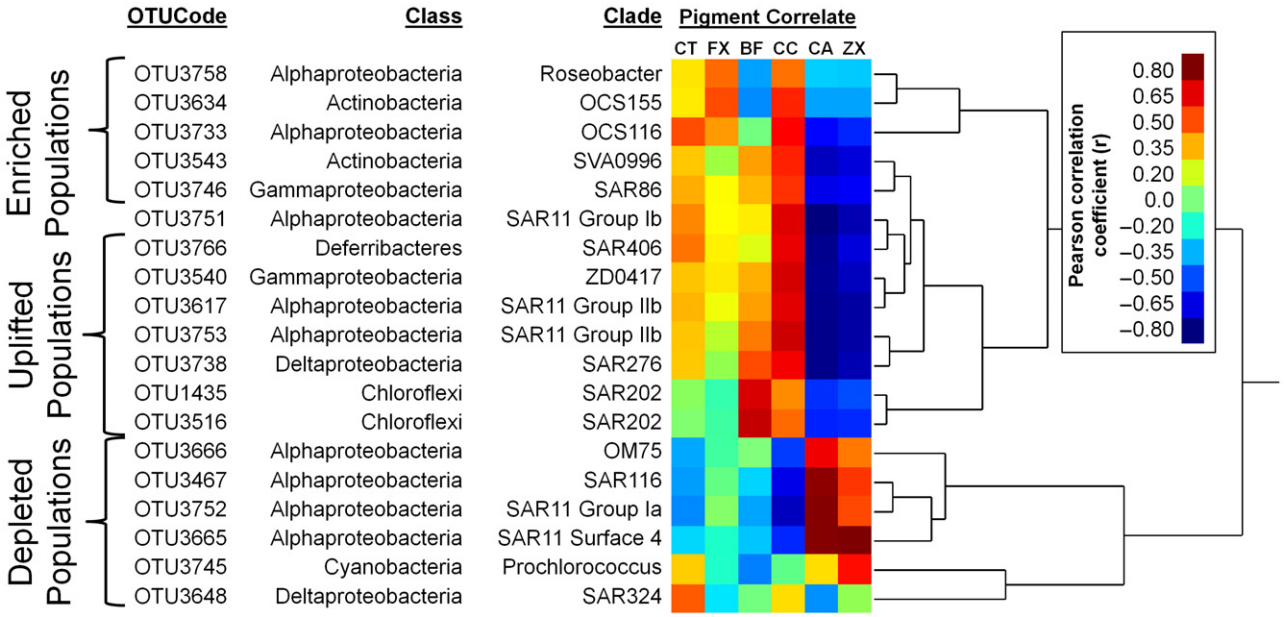

Fig. 9. Clustering of OTUs according to the magnitude and direction of covariation with phytoplankton pigments. Abundant and significant OTUs (Fig. 7, Table S2) are hierarchically clustered according to Pearson correlations (r) with concentrations of phytoplankton pigments which differed between eddy edge and eddy centre (Fig. 8). Raw values of Pearson's correlation coefficient are colour-coded in a corresponding heatmap legend. The OTUs are bracketed at left according to the depth distribution patterns organized in Fig. 7 to emphasize how covariation with phytoplankton may explain depth distributions and eddy responses of particular bacterioplankton taxa.

Discussion

It is now well established that the ocean is home to thousands of bacterioplankton taxa, the majority of which are uncultivated and only distantly related to their nearest cultured relative (Rappé and Giovannoni, 2003). Developing an understanding of the ecology and basic life histories of these organisms requires synthesis of experiments and *in situ* observations of their distributions and response to environmental change. Examining population distributions across an eddy in the context of enhanced productivity is an excellent starting point for inferring fundamental ecological characteristics of specific bacterial taxa and their role in oceanic biogeochemistry. This study represents the first complete snapshot of the effect of a mesoscale eddy feature on the distribution of genus-level bacterial populations in the ocean. By simultaneously analysing changes in relative abundance of hundreds of bacterial populations in response to a biogeochemically characterized environmental disturbance, this study provides a broad glimpse into the potential lifestyles of many of these uncultured organisms.

Bacterial populations responding to enhanced productivity within the eddy core

Our finding of consistent enrichment of OTUs belonging to the Roseobacter OCT lineage, marine group Actinobacteria (Acidimicrobiales clades OCS155 and SVA0996) and OCS116 lineages within the depth horizon of elevated productivity at the eddy core supports previous environmental associations of these clades with phytoplankton blooms and/or phytoplankton depth maxima in oceanic surveys. At the BATS site, both Morris and colleagues (2005) and Treusch and colleagues (2009) reported spatial and temporal associations of these three lineages with phytoplankton, either within the deep chlorophyll maximum or with winter blooms associated with deep mixing. Recently, Morris and colleagues (2012) reported increases in the relative abundance of members of these three lineages along horizontal and vertical gradients in chlorophyll *a* in a transect survey of the South Atlantic gyre (note that the OM1 and OCS155 designations for the marine group Actinobacteria are synonymous; Rappé *et al.*, 1999). The established associations of these clades with elevated phytoplankton biomass and productivity in time (Morris *et al.*, 2005; Treusch *et al.*, 2009), space (Morris *et al.*, 2012) and in response to a bloom-inducing eddy (shown here) suggest that these clades exhibit a meso-oligotrophic lifestyle: inhabiting unproductive regions of the ocean but consistently tracking and responding to transient hotspots of productivity. These clades may share characteristics which enable a life history strategy distinct from more traditional copiotrophs (*sensu* Lauro *et al.*, 2009), allowing these clades to dominate resource pulses in oligotrophic

habitats yet remain somewhat abundant and widespread in the absence of such pulses.

It is also notable that we did not observe enrichment of bacterial clades traditionally associated with copiotrophic lifestyles and rapid response to resource pulses within the eddy centre. Organisms belonging to the traditionally copiotrophic Gammaproteobacterial clades Alteromonas, Vibrio and Marinobacter exhibited low relative abundances consistent with background levels in the Sargasso Sea and no significant differences between eddy edge and eddy centre (see Fig. S2). These organisms are rare in the environment but commonly observed to numerically dominate communities in response to dissolved organic matter (DOM) resource pulses in experiments from diverse marine habitats (e.g. Carlson, 2002; McCarren *et al*., 2010; Nelson and Carlson, 2012; Sarmento and Gasol, 2012) and shown to rapidly assimilate phytoplankton organic matter (Nelson and Carlson, 2012); their absence of response to the eddy suggests either a temporal mismatch between their response and the time of sampling or rapid removal by top-down pressures (grazing or viral lysis).

The Roseobacter clade is one of the best characterized marine bacterioplankton, with many cultured representatives, and is often found in association with surfaces, high abundances of phytoplankton, areas of elevated productivity or benthic organisms (Buchan *et al*., 2005). Our results indicate that the member of the OCT lineage of Roseobacter enhanced within the eddy core is responding to the elevated diatom biomass and productivity, consistent with members of this subclade specializing in coastal areas and colder climates with more abundant phytoplankton associations (Buchan *et al*., 2005). Members of the Roseobacter clade have also been linked to metabolism of reduced sulfur compounds (González *et al*., 2000; Moran *et al*., 2003; Malmstrom *et al*., 2004; Buchan *et al*., 2005; Wagner-Döbler and Biebl, 2006), and there is increasing evidence that diatoms can be significant sources of reduced sulfur (Stefels, 2000; Tison *et al*., 2010; Franklin *et al*., 2012; Spielmeyer and Pohnert, 2012). Bailey and colleagues (2008) found elevated concentrations of dimethylsulfide within Eddy A4 relative to the surrounding water and a nearby cyclonic eddy, suggesting that the source may have been the degradation of phytoplankton osmolytes by Roseobacter within the eddy core (Wagner-Döbler and Biebl, 2006).

The fourth OTU enhanced within the eddy core, the Gammaproteobacteria SAR86 clade, is another uncultivated lineage typically associated with a free-living oligotrophic lifestyle in the stratified euphotic zone (Giovannoni and Vergin, 2012) with distributions similar to that of the abundant Pelagibacteraceae (a member of the SAR11 Group Ia). However, recent genomic evidence suggests that the streamlined genome of SAR86 maintains additional capabilities to metabolize reduced sulfur compounds such as glutathione and dimethylsulfoniopropionate (DMSP) (Dupont *et al*., 2012), potentially enabling the organism to respond to such compounds within the eddy core.

Additional bacterial populations differentially distributed within and outside eddies

This study represents a major advance in our ability to visualize which bacterial taxa are enhanced in the productive eddy core, which are physically displaced by isopycnal uplift, and which exhibit reduced relative abundance within the eddy. Decades of work examining the spatial and temporal distributions of bacterioplankton at the BATS site have established that community structure associates strongly with either photic or aphotic distributions in the vertically stratified water column (Gordon and Giovannoni, 1996; Field *et al*., 1997; Morris *et al*., 2005; Carlson *et al*., 2008; Treusch *et al*., 2009; Giovannoni and Vergin, 2012). Our results confirm this and clearly demonstrate the strong effect of depth on community structure (Fig. 5; MDS ordination axis 1). Organisms such as the Chloroflexi SAR202 (Morris *et al*., 2004), Deferribacteres SAR406 (Gordon and Giovannoni, 1996), Deltaproteobacteria SAR324 (Wright *et al*., 1997) and the mesopelagic Group IIb subclades of the Alphaproteobacteria SAR11 (Carlson *et al*., 2008; Vergin *et al*., 2013) all exhibit orders of magnitude increased abundance below the euphotic zone in the Sargasso Sea, with little seasonal fluctuation (Treusch *et al*., 2009), and can thus be used as reliable tracers of water masses originating from the mesopelagic realm. We observed each of these clades statistically enriched within the eddy centre relative to the eddy edge, with enrichment most pronounced at depths below those associated with the productivity response (i.e. below 100 m) and most highly correlated with distributions of inorganic nitrogen in the water ($r > 0.5$).

The suite of OTUs significantly reduced in relative abundance within the eddy centre included members of the three most abundant bacterial clades in the stratified euphotic waters of the Sargasso Sea: the Alphaproteobacteria SAR11 Group Ia, the Alphaproteobacteria SAR116 Group Ia and the Cyanobacteria Prochlorococcus. These organisms are well-established oligotrophs, with cultured representatives all exhibiting minimalist genomes, small cell size and metabolic adaptations to low-nutrient, high-light environments (Rocap *et al*., 2003; Giovannoni *et al*., 2005; Oh *et al*., 2010; Vergin *et al*., 2013). We also observed depletion of the poorly characterized Alphaproteobacteria OM75 clade, a group of organisms widespread in the surface oceans (Rappé *et al*., 1999; Suzuki *et al*., 2004; DeLong *et al*., 2006). Their distribution and depletion within the eddy core

suggest that this organism may also be a free-living oligotroph analogous to SAR11 or SAR86; but with no cultured representatives or sequenced genomic scaffolds to test this hypothesis, we cannot speculate further.

Interestingly, we identified two different OTUs belonging to the SAR324 clade that exhibited significant differences between the eddy core and eddy edge, but the two OTUs appeared to respond differently to the eddy. The more abundant OTU3738 belongs to the SAR324 Group I subclade (Brown and Donachie, 2007), most closely matching GenBank accession AY923026, and appears here to be a mesopelagic organism uplifted along pycnoclines into the eddy core. The less abundant OTU3648 associates with the recently identified SAR276 subclade of SAR324 (Brown and Donachie, 2007), most closely matching GenBank accession U65915, and is depleted within the eddy core. Brown and Donachie (2007) show that these two clades cohabitate in the euphotic and upper mesopelagic zones of tropical waters (above 250 m) and suggest that they do so by maintaining some niche segregation, which our results support by demonstrating differential association with the eddy centre and edge respectively. The recent sequencing and assembly of an uncultivated genome belonging to a distant subclade of SAR324 from coastal waters (6 m depth near La Jolla, California; Chitsaz *et al.*, 2011) revealed genomic features associated with a highly motile lifestyle and aerobic chemoheterotrophic metabolism consistent with the degradation of sinking photosynthetic biomass as might be expected in the upper mesopelagic or in coastal habitats.

Biogeochemical and community responses to the eddy

This study builds extensively on prior work establishing broader patterns of microbial community dynamics in mesoscale features. Ewart and colleagues (2008) provided the central context, demonstrating enhanced bacterial thymidine incorporation and biomass coincident with elevated chlorophyll *a*, primary production and diatom concentrations in Eddy A4. Here we expand on this dataset using a new statistical approach to more clearly define where in the water column the eddy centre departs from values outside of the eddy, additionally demonstrating significant enhancement in bacterial ^{3}H-leucine incorporation, POC concentrations and accessory pigment concentrations within the same 60–100 m depth horizon of the eddy core and showing that these are consistent with a localized response rather than a physical displacement (Fig. 3). These results support the interpretation of bacterioplankton communities responding to increased primary production, particulate organic matter and changing phytoplankton communities within the eddy core, with responses including shifts in production, biomass, community structure (Figs 4–5), diversity (Fig. 6) and population enrichment (Fig. 7).

These companion studies mark an important step forward because of the resolution of the eddy with more than 10 profiles; prior work on eddy microbiology has been limited to just one or two profiles in each mesoscale feature, significantly limiting statistical power to test differences within and outside of the eddies. Baltar and colleagues (2010) observed increased bacterial abundances and ^{3}H-leucine incorporation within both cyclonic and anticyclonic eddies relative to outside stations within the euphotic and mesopelagic zones. They further observed community patterns in the euphotic, mesopelagic and bathypelagic zones inside and outside of the eddies, with indications that euphotic community differences between the eddy and outside stations were greatest. Zhang and colleagues (2009) extended this work to investigate domain-level patterns in community structure of cyclonic eddies in the South China Sea using fluorescence in situ hybridization microscopy to count Eubacteria, Crenarchaeota and Euryarchaeota. They indicated increased abundance of Crenarchaeota within eddy profiles and elevated incorporation of D-aspartic acid within the cyclonic eddies. In a companion study, Zhang and colleagues (2011) found that the deep waters beneath cyclonic eddies exhibited a vertical expansion of the distribution of communities with a mesopelagic signature, likely due to isopycnal uplift, corroborating our observations. Given these results, it would be interesting to examine patterns of both bacterial and archaeal community differentiation within the mesopelagic and bathypelagic zones beneath the productive core of anticyclonic eddies, especially given the dramatic oxygen minima observed between 800 and 1000 m below Eddy A4 (McGillicuddy *et al.*, 2007) and evidence for eddies driving mesopelagic microbial community dynamics in the North Atlantic (Baltar *et al.*, 2012).

Conclusions

Previous work in the Sargasso Sea has demonstrated systematic broad-scale variability in bacterioplankton community structure over depth and through time (Gordon and Giovannoni, 1996; Field *et al.*, 1997; Morris *et al.*, 2005; Carlson *et al.*, 2008; Treusch *et al.*, 2009; Giovannoni and Vergin, 2012). Here we have demonstrated systematic submesocale variability in the bacterioplankton community structure in both horizontal and vertical space across an anticyclonic MWE. Using *a priori* physical and chemical definitions to differentiate eddy edge and eddy centre, we use rigorous statistical approaches (repeated measures MANOVA and false discovery rate controls) to identify bacterial populations that are differentially enriched or depleted across depths

within the eddy. By examining these taxon distributions, we can derive insight into the various mechanisms driving community shifts, specifically differentiating those taxa which are responding to eddy productivity (e.g. those enriched coincident with eddy core biogeochemical responses) from those taxa which are physically entrained into the eddy. By linking these patterns with pigment distributions and a wealth of biogeochemical context from prior research, we can infer something of the ecology of these uncultured lineages, allowing further generation of hypotheses regarding the life histories and biogeochemical roles of the massive diversity of bacteria in the world's oceans.

Experimental procedures

Eddy context and sampling scheme

The present work was conducted as part of a large interdisciplinary programme designed to track the physical, chemical and biological characteristics of mesoscale eddy features in the northwestern subtropical Atlantic Ocean: EDDIES (EDdy Dynamics, mixing, Export and Species composition). Here we focus on Eddy A4, an anticyclonic MWE sampled during six cruises from June to October of 2005. Samples for the present study were collected during two eddy occupations aboard the *R/V Weatherbird II*: WBII X0506 (6–15 July 2005) and WBII X0508 (16–25 August 2005). Much of the physical, biological and chemical data collected on these cruises has been reported previously (McGillicuddy *et al*., 2007; Benitez-Nelson and McGillicuddy, 2008) and is available online from the Ocean Carbon and Biogeochemistry Data System (http://ocb.whoi.edu/jg/dir/OCB/EDDIES/).

The dataset used here consisted of 19 profiles from the July occupation (Fig. 1) and an additional 3 profiles from the August occupation. Data regarding bacterioplankton biomass and activity within this MWE have been previously reported by Ewart and colleagues (2008). In the present study, a subset of 11 profiles collected on these cruises was analysed further for bacterial community composition via 16S amplicon pyrosequencing (annotated with asterisks in Figs 1 and 2). Briefly, we selected a subset of 10 eddy-associated profiles over five depths ranging from 40 to 120 m for 16S pyrosequencing: seven profiles from the July occupation, including two from the eddy centre and three profiles from the eddy centre during the August occupation. We included a synoptic profile of the nearby BATS station as an external reference.

Sample collection and storage

Water samples (2 l) were collected from rosette Niskin bottles (Ocean Test Equipment, Fort Lauderdale, FL, USA) into 4 l tubulated polyethylene bottles that had been acid-washed (5% HCl), Milli-Q water (Millipore, Billerica, MA, USA) rinsed and triple-rinsed with sample water prior to each collection. Sequential 47 mm polyethersulfone filters (SUPOR-200; 1.2 μm and 0.2 μm; Pall Corporation, Port Washington, NY, USA) were placed in-line within polycarbonate filter holders and attached directly to the sample bottles. Water was drawn under vacuum at 150 mm Hg. Filters were rolled with ethanol-cleaned forceps and placed in sterile 5 ml cryovials containing 1.5 ml sucrose lysis buffer (20 mmol l^{-1} EDTA/ 400 mmol l^{-1} NaCl/750 mmol l^{-1} sucrose/50 mmol l^{-1} Tris-HCL, pH 9.0) and frozen immediately in liquid nitrogen, with long-term storage at –80°C until further processing. Upon thawing, cells were lysed to release DNA into solution by adding sodium dodecyl sulfate (1%) and Proteinase K (0.2 mg ml^{-1}) to each cryovial and incubating 10 h at 57°C. Genomic DNA was extracted from a 250 μl aliquot of this lysate (roughly equivalent to 300 ml of filtered sample water) using a commercial silica column centrifugation kit (DNEasy, Qiagen, Valencia, CA, USA). The extracted DNA from the 0.2 μm filters only was used as template for polymerase chain reaction (PCR) amplification of regions of the gene encoding the 16S ribosomal RNA subunit for bacterial taxonomic analyses. We conducted multiplex amplicon pyrosequencing (Hamady *et al*., 2008); libraries were constructed and processed according to Nelson and Carlson (2012) using primers targeting the V1 and V2 hypervariable regions of the 16S gene. PCR reactions used 2 μl template (equivalent to DNA from 100 ml sample water) in a 25 μl reaction mixture containing 1.5 Unit PerfectTaq Polymerase (5Prime, Gaithersburg, MD, USA) in proprietary buffer, 50 nM each dNTP, 2.5 mmol l^{-1} additional MgCl2 (4 mmol l^{-1} final), 5% Acetamide and 200 nM each forward and reverse primers. Primers used were forward primer 8f (with 5′ Roche FLX Amplicon Adapter B GCCTTGCCAGCCCGCTCAG followed by TC linker) and reverse primer 338r (TGCWGC CWCCCGTAGGWGT with 5′ Roche FLX Amplicon Adapter A and integrated barcode GCCTCCCTCGCGCCATCAG xxxxxxxxCA, where x's refer to oligonucleotide 'barcodes'; Hamady *et al*., 2008). PCR reaction conditions were 270 s 94°C hotstart, 35 cycles of 30 s 94°C, 60 s 57°C, 120 s 72°C, 600 s 72°C extension. After cleaning the PCRs (Wizard 96, Promega, Madison, WI, USA), DNA was quantified using SYBR Green I and PCR products were pooled in equimolar proportions before agarose gel electrophoresis separation and subsequent extraction (QiaEx; Qiagen, Germantown, MD, USA). Pyrosequencing runs are deposited in the NCBI Sequence Read Archive (http://trace.ncbi.nlm.nih.gov/Traces/sra) as run accession SRR828415, with multiplexing barcodes listed in Table S1.

16S sequence processing and analysis

Sequence analysis was conducted primarily within the open-source software framework mothur (v 1.27; Schloss *et al*., 2009) using a previously described bioinformatic pipeline (Nelson and Carlson, 2012) updated with recently released algorithms where noted below. First, pyrosequencer flowgrams were quality-controlled for sequencing error using PyroNoise (Quince *et al*., 2009), and PCR-based chimeras were identified and removed using Perseus (Quince *et al*., 2011) as were sequences with ambiguous bases, long homopolymers ($n > 6$) or short reads (< 200 bp). Sequences were aligned using mothur to a non-redundant subset of the most recent (v111) SILVA SSU Ref 16S curated alignment database (Quast *et al*., 2012) modified to approximate the proprietary SILVA SEED alignment beginning with the

recommendations of Schloss (2010). Briefly, the SILVA SSU_Refv111 alignment was reduced to sequences with 100% alignment quality, > 85% sequence quality, > 1100 bp length and < 0.5% ambiguous bases. To ensure inclusion of representative high-quality sequences from all annotated phylotypes, this alignment was supplemented with sequences from the dereplicated SILVA SSU_Ref_NRv111 database containing a unique phylogenetic identification string not in the Refv111 subset using the same criteria but with relaxed (> 99%) alignment quality. This alignment was then manually curated to remove identical sequences, misaligned sequences, non-bacterial/plastid sequences and rare variants that created large gaps in the alignment (roughly 0.005%). This final template alignment was filtered to remove common gaps, containing 65 358 sequences and spanning 6093 positions.

Following alignment sequences were quality-controlled for single-base PCR substitution errors using centroid-based single-linkage preclustering (Huse *et al*., 2010). Sequences were preliminarily classified from this alignment under the SILVA taxonomy (Pruesse *et al*., 2007) using the Bayesian classification algorithm of Wang and colleagues (2007). Sequences were assigned to OTUs via average-neighbour hierarchical clustering at the 95% identity level (95% identity over the V1-V2 region best approximates the 97% identity level of the full-length 16S gene commonly used to delineate OTUs; Schloss, 2010), and OTUs were then consensus classified at the 70% confidence level. Final classification assignments of common OTUs were verified via hidden Markov model-based alignment (Eddy, 2011) and phylogenetic placement (Matsen *et al*., 2010) within a manually curated maximum-likelihood phylogeny of marine bacterioplankton using the PhyloAssigner pipeline (Vergin *et al*., 2013). Diversity metrics were calculated within mothur for each sample based on sequence abundance within each OTU (rarefied by random subsampling at 700 sequences per sample). UniFrac (Lozupone and Knight, 2005) was used to calculate phylogenetic distances between samples from an abundance-weighted maximum-likelihood phylogeny constructed from an alignment of one representative sequence from each OTU with RAxML software (v 7.3.2; Stamatakis, 2006) via the CIPRES web portal (Miller *et al*., 2010).

Statistical analyses

All statistics were conducted using SAS via the JMP software package (Version 10. SAS Institute Inc., Cary, NC, USA, 1989–2012) unless otherwise noted. To test each bacterial OTU population or environmental measurement for statistical differences between eddy edge (6 profiles, 29 samples) and eddy centre (5 profiles, 25 samples) over five depths (40, 60, 80, 100 and 120 m), we used a repeated measures design of MANOVA with depth as the repeated measure (sometimes called profile analysis; O'Brien and Kaiser, 1985; Scheiner and Gurevitch, 2001). The repeated measures design is most appropriate and conservative for this analysis because it accounts for dependence between different sampling depths within individual station profiles. In addition, by comparing mean profile 'shapes' between locations (eddy edge vs. eddy centre), the repeated measures design distinguishes if locations differ in overall OTU relative abundances across depths (i.e. testing for a significant location effect) and/or if the locations differ in their OTU distributions among depths (i.e. testing for a significant location*depth interaction). Variables with significant between-subjects location effects (eddy edge vs. eddy centre; $p_e < 0.05$) or significant within-subjects interaction effects (eddy location*depth; $p_{e*d} < 0.05$) were interpreted as differing within the eddy centre relative to the eddy edge and BATS stations; model intercepts and within-subjects depth effects were always significant ($P < 0.05$) as expected and are not discussed further.

To correct for multiple comparisons (e.g. testing of multiple individual OTUs for significant differences between eddy edge and eddy centre), we controlled the false discovery rate to reduce the number of false positive discoveries to less than 1 at the alpha = 0.05 level using the q-value approach of Storey and Tibshirani (2003) as coded in JMP by Osborne and Barker (2007) (i.e. q * # of significant tests < 1). OTU and pigment relative abundances were arcsin (square root) transformed to best approximate the Gaussian (normal) distribution before all MANOVA tests and other linear modelling. Hierarchical clustering was performed on untransformed data using the complete-linkage algorithm in JMP. MDS ordination of samples according to UniFrac distances and similarity profiling (SIMPROF) and ANOSIM algorithms were run using the software package PRIMER (v 6; Clarke and Gorley, 2006). Contour plots were generated with Ocean Data View (Schlitzer, 2002).

Acknowledgements

The authors wish to thank Dennis McGuillicuddy and Rodney Johnson for their excellent leadership, planning logistics and valuable insights into eddy dynamics. We thank the captain, crew and scientists aboard the R.V. *Weatherbird II* for their valuable assistance during the cruises. We thank Meredith Meyers and Stuart Halewood for valuable technical assistance. This manuscript benefited from interactions with students of the BIOS Microbial Oceanography summer course and from discussions with Kevin Vergin regarding PhyloAssigner. This work was supported by National Science Foundation Biological Oceanography OCE 0425615, the Emerging Topics in Biogeochemistry program OCE-0801991 and the Gordon and Betty Moore Foundation's Marine Microbiology Initiative program to C.A.C. This is publication 8989 of the University of Hawai'i School of Ocean and Earth Science and Technology (SOEST).

References

Bailey, K.E., Toole, D.A., Blomquist, B., Najjar, R.G., Huebert, B., Kieber, D.J., *et al*. (2008) Dimethylsulfide production in Sargasso Sea eddies. *Deep Sea Res Part II Top Stud Oceanogr* **55:** 1491–1504.

Baltar, F., Arístegui, J., Gasol, J.M., Lekunberri, I., and Herndl, G.J. (2010) Mesoscale eddies: hotspots of prokaryotic activity and differential community structure in the ocean. *ISME J* **4:** 975–988.

Baltar, F., Arístegui, J., Gasol, J.M., and Herndl, G.J. (2012) Microbial functioning and community structure variability in the mesopelagic and epipelagic waters of the subtropical Northeast Atlantic Ocean. *Appl Environ Microbiol* **78:** 3309–3316.

Benitez-Nelson, C.R., and McGillicuddy, D.J., Jr (2008) Mesoscale physical–biological–biogeochemical linkages in the open ocean: an introduction to the results of the E-Flux and EDDIES programs. *Deep Sea Res Part II Top Stud Oceanogr* **55:** 1133–1138.

Bibby, T.S., Gorbunov, M.Y., Wyman, K.W., and Falkowski, P.G. (2008) Photosynthetic community responses to upwelling in mesoscale eddies in the subtropical North Atlantic and Pacific Oceans. *Deep Sea Res Part II Top Stud Oceanogr* **55:** 1310–1320.

Brown, M.V., and Donachie, S. (2007) Evidence for tropical endemicity in the Deltaproteobacteria Marine Group B/SAR324 bacterioplankton clade. *Aquat Microb Ecol* **46:** 107–115.

Buchan, A., González, J.M., and Moran, M.A. (2005) Overview of the marine Roseobacter lineage. *Appl Environ Microbiol* **71:** 5665–5677.

Buesseler, K.O., Lamborg, C., Cai, P., Escoube, R., Johnson, R., Pike, S., *et al*. (2008) Particle fluxes associated with mesoscale eddies in the Sargasso Sea. *Deep Sea Res Part II Top Stud Oceanogr* **55:** 1426–1444.

Bunge, J. (2011) Estimating the number of species with catchall. *Pac Symp Biocomput***:** 121–130.

Carlson, C.A. (2002) Production and removal processes. In *Biogeochemistry of Marine Dissolved Organic Matter*. Hansell, D.A., and Carlson, C.A. (eds). San Diego: Academic Press, pp. 91–151.

Carlson, C.A., Morris, R., Parsons, R., Treusch, A.H., Giovannoni, S.J., and Vergin, K. (2008) Seasonal dynamics of SAR11 populations in the euphotic and mesopelagic zones of the northwestern Sargasso Sea. *ISME J* **3:** 283–295.

Chao, A. (1984) Nonparametric estimation of the number of classes in a population. *Scand J Stat* **11:** 265–270.

Chitsaz, H., Yee-Greenbaum, J.L., Tesler, G., Lombardo, M.-J., Dupont, C.L., Badger, J.H., *et al*. (2011) Efficient de novo assembly of single-cell bacterial genomes from short-read data sets. *Nat Biotechnol* **29:** 915–921.

Clarke, K., and Gorley, R. (2006) PRIMER v6. User manual/tutorial. Plymouth routine in mulitvariate ecological research. Plymouth Marine Laboratory.

DeLong, E.F., Preston, C.M., Mincer, T., Rich, V., Hallam, S.J., Frigaard, N.U., *et al*. (2006) Community genomics among stratified microbial assemblages in the ocean's interior. *Science* **311:** 496–503.

Ducklow, H.W. (1999) The bacterial component of the oceanic euphotic zone. *FEMS Microbiol Ecol* **30:** 1–10.

Dupont, C.L., Rusch, D.B., Yooseph, S., Lombardo, M.-J., Richter, R.A., Valas, R., *et al*. (2012) Genomic insights to SAR86, an abundant and uncultivated marine bacterial lineage. *ISME J* **6:** 1186–1199.

Eddy, S.R. (2011) Accelerated profile HMM searches. *PLoS Comput Biol* **7:** e1002195.

Eppley, R.W., and Peterson, B.J. (1979) Particulate organic matter flux and planktonic new production in the deep ocean. *Nature* **282:** 677–680.

Ewart, C.S., Meyers, M.K., Wallner, E.R., McGillicuddy, D.J., and Carlson, C.A. (2008) Microbial dynamics in cyclonic and anticyclonic mode-water eddies in the northwestern Sargasso Sea. *Deep Sea Res Part II Top Stud Oceanogr* **55:** 1334–1347.

Field, K.G., Gordon, D., Wright, T., Rappé, M., Urback, E., Vergin, K., and Giovannoni, S.J. (1997) Diversity and depth-specific distribution of SAR11 cluster rRNA genes from marine planktonic bacteria. *Appl Environ Microbiol* **63:** 63.

Franklin, D.J., Airs, R.L., Fernandes, M., Bell, T.G., Bongaerts, R.J., and Berges, J.A. (2012) Identification of senescence and death in *Emiliania huxleyi* and *Thalassiosira pseudonana*: cell staining, chlorophyll alterations, and dimethylsulfoniopropionate (DMSP) metabolism. *Limnol Oceanogr* **57:** 305.

Giovannoni, S.J., and Vergin, K.L. (2012) Seasonality in ocean microbial communities. *Science* **335:** 671–676.

Giovannoni, S.J., Tripp, H.J., Givan, S., Podar, M., Vergin, K.L., Baptista, D., *et al*. (2005) Genome streamlining in a cosmopolitan oceanic bacterium. *Science* **309:** 1242–1245.

Goldthwait, S.A., and Steinberg, D.K. (2008) Elevated biomass of mesozooplankton and enhanced fecal pellet flux in cyclonic and mode-water eddies in the Sargasso Sea. *Deep Sea Res Part II Top Stud Oceanogr* **55:** 1360–1377.

González, J.M., Simó, R., Massana, R., Covert, J.S., Casamayor, E.O., Pedrós-Alió, C., and Moran, M.A. (2000) Bacterial community structure associated with a dimethylsulfoniopropionate-producing North Atlantic algal bloom. *Appl Environ Microbiol* **66:** 4237–4246.

Gordon, D.A., and Giovannoni, S.J. (1996) Detection of stratified microbial populations related to Chlorobium and Fibrobacter species in the Atlantic and Pacific Oceans. *Appl Environ Microbiol* **62:** 1171.

Hamady, M., Walker, J.J., Harris, J.K., Gold, N.J., and Knight, R. (2008) Error-correcting barcoded primers for pyrosequencing hundreds of samples in multiplex. *Nat Methods* **5:** 235–237.

Huse, S.M., Welch, D.M., Morrison, H.G., and Sogin, M.L. (2010) Ironing out the wrinkles in the rare biosphere through improved OTU clustering. *Environ Microbiol* **12:** 1889–1898.

Jenkins, W.J., and Doney, S.C. (2003) The subtropical nutrient spiral. *Global Biogeochem Cycles* **17:** 1110.

Jenkins, W.J., Webb, D.J., Merlivat, L., and Roether, W. (1988) The use of anthropogenic Tritium and Helium-3 to study subtropical gyre ventilation and circulation [and discussion]. *Philos Trans R Soc Lond A* **325:** 43–61.

Jenkins, W.J., McGillicuddy, D.J. Jr, and Lott, D.E. III (2008) The distributions of, and relationship between, ^{3}He and nitrate in eddies. *Deep Sea Res Part II Top Stud Oceanogr* **55:** 1389–1397.

Lauro, F.M., McDougald, D., Thomas, T., Williams, T.J., Egan, S., Rice, S., *et al*. (2009) The genomic basis of trophic strategy in marine bacteria. *Proc Natl Acad Sci U S A* **106:** 15527–15533.

Ledwell, J.R., McGillicuddy, D.J., and Anderson, L.A. (2008) Nutrient flux into an intense deep chlorophyll layer in a mode-water eddy. *Deep Sea Res Part II Top Stud Oceanogr* **55:** 1139–1160.

Li, Q.P., and Hansell, D.A. (2008) Nutrient distributions in baroclinic eddies of the oligotrophic North Atlantic and inferred impacts on biology. *Deep Sea Res Part II Top Stud Oceanogr* **55:** 1291–1299.

Lozupone, C., and Knight, R. (2005) UniFrac: a new phylogenetic method for comparing microbial communities. *Appl Environ Microbiol* **71:** 8228–8235.

McCarren, J., Becker, J.W., Repeta, D.J., Shi, Y., Young, C.R., Malmstrom, R.R., *et al*. (2010) Microbial community transcriptomes reveal microbes and metabolic pathways associated with dissolved organic matter turnover in the sea. *PNAS* **107:** 16420–16427.

McGillicuddy, D.J., Johnson, R., Siegel, D.A., Michaels, A.F., Bates, N.R., and Knap, A.H. (1999) Mesoscale variations of biogeochemical properties in the Sargasso Sea. *J Geophys Res: Oceans* **104:** 13381–13394.

McGillicuddy, D.J., Anderson, L.A., Bates, N.R., Bibby, T., Buesseler, K.O., Carlson, C.A., *et al*. (2007) Eddy/wind interactions stimulate extraordinary mid-ocean plankton blooms. *Science* **316:** 1021–1026.

Malmstrom, R.R., Kiene, R., and Kirchman, D.L. (2004) Identification and enumeration of bacteria assimilating dimethylsulfoniopropionate (DMSP) in the North Atlantic and Gulf of Mexico. *Limnol Oceanogr* **49:** 597–606.

Matsen, F.A., Kodner, R.B., and Armbrust, E.V. (2010) pplacer: linear time maximum-likelihood and Bayesian phylogenetic placement of sequences onto a fixed reference tree. *BMC Bioinformatics* **11:** 538.

Miller, M.A., Pfeiffer, W., and Schwartz, T. (2010) Creating the CIPRES Science Gateway for inference of large phylogenetic trees. In *Proceedings of the Gateway Computing Environments Workshop (GCE)*, 14 November 2010, New Orleans, LA. pp. 1–8.

Moran, M.A., Gonzalez, J.M., and Kiene, R. (2003) Linking a bacterial taxon to sulfur cycling in the sea: studies of the marine Roseobacter group. *Geomicrobiol J* **20:** 375–388.

Morris, R.M., Rappé, M.S., Urbach, E., Connon, S.A., and Giovannoni, S.J. (2004) Prevalence of the Chloroflexi-Related SAR202 Bacterioplankton cluster throughout the mesopelagic zone and deep ocean. *Appl Environ Microbiol* **70:** 2836–2842.

Morris, R.M., Vergin, K.L., Cho, J.C., Rappé, M.S., Carlson, C.A., and Giovannoni, S.J. (2005) Temporal and spatial response of bacterioplankton lineages to annual convective overturn at the Bermuda Atlantic Time-series Study site. *Limnol Oceanogr* **50:** 1687–1696.

Morris, R.M., Frazar, C.D., and Carlson, C.A. (2012) Basin-scale patterns in the abundance of SAR11 subclades, marine Actinobacteria (OM1), members of the Roseobacter clade and OCS116 in the South Atlantic. *Environ Microbiol* **14:** 1133–1144.

Nelson, C.E. (2009) Phenology of high-elevation pelagic bacteria: the roles of meteorologic variability, catchment inputs and thermal stratification in structuring communities. *ISME J* **3:** 13–30.

Nelson, C.E., and Carlson, C.A. (2012) Tracking differential incorporation of dissolved organic carbon types among diverse lineages of Sargasso Sea bacterioplankton. *Environ Microbiol* **14:** 1500–1516.

O'Brien, R.G., and Kaiser, M.K. (1985) MANOVA method for analyzing repeated measures designs: an extensive primer. *Psychol Bull* **97:** 316–333.

Oh, H.-M., Kwon, K.K., Kang, I., Kang, S.G., Lee, J.-H., Kim, S.-J., and Cho, J.-C. (2010) Complete genome sequence of '*Candidatus Puniceispirillum marinum*' IMCC1322, a representative of the SAR116 clade in the *Alphaproteobacteri*a. *J Bacteriol* **192:** 3240–3241.

Osborne, J.A., and Barker, C.A. (2007) Estimating the false discovery rate using using SAS r and JMP r. *The Proceedings of the SouthEast SAS Users Group*. Proceedings of the SESUG.

Pruesse, E., Quast, C., Knittel, K., Fuchs, B.M., Ludwig, W., Peplies, J., and Glöckner, F.O. (2007) SILVA: a comprehensive online resource for quality checked and aligned ribosomal RNA sequence data compatible with ARB. *Nucleic Acids Res* **35:** 7188 –7196.

Quast, C., Pruesse, E., Yilmaz, P., Gerken, J., Schweer, T., Yarza, P., *et al*. (2012) The SILVA ribosomal RNA gene database project: improved data processing and web-based tools. *Nucleic Acids Res* **41:** D590–D596.

Quince, C., Lanzén, A., Curtis, T., Davenport, R.J., Hall, N., Head, I.M., *et al*. (2009) Accurate determination of microbial diversity from 454 pyrosequencing data. *Nat Methods* **6:** 639–641.

Quince, C., Lanzen, A., Davenport, R.J., and Turnbaugh, P.J. (2011) Removing noise from Pyrosequenced Amplicons. *BMC Bioinformatics* **12:** 38.

Rappé, M.S., and Giovannoni, S.J. (2003) The uncultured microbial majority. *Annu Rev Microbiol* **57:** 369–394.

Rappé, M.S., Gordon, D.A., Vergin, K.L., and Giovannoni, S.J. (1999) Phylogeny of Actinobacteria Small Subunit (SSU) rRNA Gene clones recovered from marine Bacterioplankton. *Syst Appl Microbiol* **22:** 106–112.

Richardson, P.L. (1993) A census of eddies observed in North Atlantic SOFAR float data. *Prog Oceanogr* **31:** 1–50.

Rocap, G., Larimer, F.W., Lamerdin, J., Malfatti, S., Chain, P., Ahlgren, N.A., *et al*. (2003) Genome divergence in two *Prochlorococcus* ecotypes reflects oceanic niche differentiation. *Nature* **424:** 1042–1047.

Sarmento, H., and Gasol, J.M. (2012) Use of phytoplankton-derived dissolved organic carbon by different types of bacterioplankton. *Environ Microbiol* **14:** 2348–2360.

Scheiner, S.M., and Gurevitch, J. (2001) *Design and Analysis of Ecological Experiments*. USA: Oxford University Press.

Schlitzer, R. (2002) Interactive analysis and visualization of geoscience data with ocean data view. *Comput Geosci* **28:** 1211–1218.

Schloss, P.D. (2010) The effects of alignment quality, distance calculation method, sequence filtering, and region on the analysis of 16S rRNA Gene-Based Studies. J.A. Eisen (ed.). *PLoS Comput Biol* **6:** e1000844.

Schloss, P.D., Westcott, S.L., Ryabin, T., Hall, J.R., Hartmann, M., Hollister, E.B., *et al*. (2009) Introducing mothur: open-source, platform-independent, community-supported software for describing and comparing microbial communities. *Appl Environ Microbiol* **75:** 7537–7541.

Siegel, D.A., McGillicuddy, D.J., and Fields, E.A. (1999) Mesoscale eddies, satellite altimetry, and new production in the Sargasso Sea. *J Geophys Res: Oceans* **104:** 13359–13379.

Spielmeyer, A., and Pohnert, G. (2012) Daytime, growth phase and nitrate availability dependent variations of dimethylsulfoniopropionate in batch cultures of the diatom Skeletonema marinoi. *J Exp Mar Bio Ecol* **413:** 121–130.

Stamatakis, A. (2006) RAxML-VI-HPC: maximum likelihood-based phylogenetic analyses with thousands of taxa and mixed models. *Bioinformatics* **22:** 2688–2690.

Stefels, J. (2000) Physiological aspects of the production and conversion of DMSP in marine algae and higher plants. *J Sea Res* **43:** 183–197.

Steinberg, D.K., Carlson, C.A., Bates, N.R., Johnson, R.J., Michaels, A.F., and Knap, A.H. (2001) Overview of the US JGOFS Bermuda Atlantic Time-series Study (BATS): a decade-scale look at ocean biology and biogeochemistry. *Deep Sea Res Part II Top Stud Oceanogr* **48:** 1405–1447.

Storey, J.D., and Tibshirani, R. (2003) Statistical significance for genomewide studies. *Proc Natl Acad Sci USA* **100:** 9440.

Suzuki, M.T., Preston, C.M., Béjà, O., Torre, J.R., Steward, G.F., and DeLong, E.F. (2004) Phylogenetic screening of ribosomal RNA gene-containing clones in bacterial artificial chromosome (BAC) Libraries from different depths in Monterey Bay. *Microb Ecol* **48:** 473–488.

Tison, J.-L, F.B., Dumont, I., and Stefels, J. (2010) High-resolution dimethyl sulfide and dimethylsulfoniopropionate time series profiles in decaying summer first-year sea ice at Ice Station Polarstern, western Weddell Sea, Antarctica. *J Geophys Res: Biogeosciences* **115:** 2156–2202. doi:10.1029/2010JG001427.

Treusch, A.H., Vergin, K.L., Finlay, L.A., Donatz, M.G., Burton, R.M., Carlson, C.A., and Giovannoni, S.J. (2009) Seasonality and vertical structure of microbial communities in an ocean gyre. *ISME J* **3:** 1148–1163.

Vergin, K.L., Beszteri, B., Monier, A., Thrash, J.C., Temperton, B., Treusch, A.H., *et al.* (2013) High-resolution SAR11 ecotype dynamics at the Bermuda Atlantic Time-series Study site by phylogenetic placement of pyrosequences. *ISME J* **7:** 1322–1332. doi:10.1038/ismej.2013.32.

Wagner-Döbler, I., and Biebl, H. (2006) Environmental biology of the marine Roseobacter Lineage. *Annu Rev Microbiol* **60:** 255–280.

Wang, Q., Garrity, G.M., Tiedje, J.M., and Cole, J.R. (2007) Naive Bayesian classifier for rapid assignment of rRNA sequences into the new bacterial taxonomy. *Appl Environ Microbiol* **73:** 5261–5267.

Wright, T.D., Vergin, K.L., Boyd, P.W., and Giovannoni, S.J. (1997) A novel delta-subdivision proteobacterial lineage from the lower ocean surface layer. *Appl Environ Microbiol* **63:** 1441–1448.

Zhang, Y., Sintes, E., Chen, J., Zhang, Y., Dai, M., Jiao, N., and Herndl, G. (2009) Role of mesoscale cyclonic eddies in the distribution and activity of Archaea and Bacteria in the South China Sea. *Aquat Microb Ecol* **56:** 65–79.

Zhang, Y., Jiao, N., Sun, Z., Hu, A., and Zheng, Q. (2011) Phylogenetic diversity of bacterial communities in South China Sea mesoscale cyclonic eddy perturbations. *Res Microbiol* **162:** 320–329.

Supporting information

Additional Supporting Information may be found in the online version of this article at the publisher's web-site:

Fig. S1. Maximum-likelihood phylogeny of marine bacterioplankton with OTUs from this study inserted using PhyloAssigner. The tree contains three leaf types: OTUs from this study are in bold, nearest neighbours from the SILVA database are in italics and the reference scaffold of Vergin *et al.* 2013 are tagged 'Vergin_Reference'.

Fig. S2. Eddy distributions of three copiotrophic lineages of *Gammaproteobacteria* commonly found in DOM amendment experiments. None of the lineages show significant differences in depth distributions between eddy edge and eddy centre and rarely exceed 0.2% of the total community.

Table S1. Details of samples selected for pyrosequencing and sequencing outcomes. For each sample, we provide details on sample collection (cruise, dates, casts, bottles, depths and spatial groupings), pyrosequencing multiplex identifiers (pyrotag barcodes) and read counts, and diversity metrics calculated after rarefaction to homogenize read counts. Each sample is annotated according to classification as eddy edge or eddy centre and also whether it is included in the spatial transect (contour heat plots in manuscript) or offset stations (line plots in manuscript) or the BATS outgroup.

Table S2. Summary of common OTUs found in the study and statistical testing of distributional differences within and outside of the eddy centre. Each OTU is presented with a consensus classification and listed according to categories of abundance, significance and, if significant and abundant, a descriptive type of response to the eddy. The top 20 OTUs are those presented in Fig. 7 and are highlighted in grey. For each OTU MANOVA, F-statistics are presented for both the main eddy effect (between-subjects) and the interaction of eddy effects with depth (within-subjects) with respective probabilities of null hypothesis acceptance (*P*-value) and likelihood of false discovery (q-value).